Review Article | Neuroimaging and Head & Neck

http://dx.doi.org/10.3348/kjr.2016.17.5.620
pISSN 1229-6929 · eISSN 2005-8330
Korean J Radiol 2016;17(5):620-632

Korean Journal of Radiology
KJR

In-Vivo Proton Magnetic Resonance Spectroscopy of 2-Hydroxyglutarate in Isocitrate Dehydrogenase-Mutated Gliomas: A Technical Review for Neuroradiologists

Hyeonjin Kim, PhD[1, 2, 3], Sungjin Kim, MS[1], Hyeong Hun Lee, BS[2], Hwon Heo, PhD[2]

[1]Department of Radiology, Seoul National University Hospital, Seoul 03080, Korea; [2]Department of Biomedical Sciences, Seoul National University, Seoul 03087, Korea; [3]Institute of Radiation Medicine, Seoul National University Medical Research Center, Seoul 03080, Korea

The diagnostic and prognostic potential of an onco-metabolite, 2-hydroxyglutarate (2HG) as a proton magnetic resonance spectroscopy (1H-MRS) detectable biomarker of the isocitrate dehydrogenase (IDH)-mutated (IDH-MT) gliomas has drawn attention of neuroradiologists recently. However, due to severe spectral overlap with background signals, quantification of 2HG can be very challenging. In this technical review for neuroradiologists, first, the biochemistry of 2HG and its significance in the diagnosis of IDH-MT gliomas are summarized. Secondly, various 1H-MRS methods used in the previous studies are outlined. Finally, wereview previous *in vivo* studies, and discuss the current status of 1H-MRS in the diagnosis of IDH-MT gliomas.

Keywords: *Proton; Magnetic resonance spectroscopy; MRS; Isocitrate dehydrogenase; 2-hydroxyglutarate; Glioma; Mutation*

INTRODUCTION

Proton magnetic resonance spectroscopy (1H-MRS) has traditionally been used in the metabolic research of gliomas and its diagnostic value is well explored (1-9). Currently, however, 1H-MRS is used only as a supplemental tool to magnetic resonance imaging (MRI) in the diagnosis of gliomas (2, 5, 9). Such limited application of 1H-MRS in the diagnosis of gliomas can be attributed to the intrinsic low concentrations of metabolites and the limited spectral signal-to-noise ratio (SNR) and dispersion at clinical field strength. In addition, lack of specificity of metabolites that are previously proposed as biomarkers of gliomas is also responsible for its low demand by neuroradiologists. In this regard, the emergence of 2-hydroxyglutarate (2HG) as an onco-metabolite overproduced in isocitrate dehydrogenase (IDH)-mutated (IDH-MT) gliomas (10-13), the substantially longer survival duration of IDH-MT glioma patients relative to those with IDH wild-type (IDH-WT) gliomas (11), and recent pioneering studies on the feasibility of non-invasive detection of 2HG by 1H-MRS (14-16), collectively, have recently drawn attention of neuroradiologists. However, due to severe spectral overlap with its background signal, the quantification of 2HG is reportedly challenging (15, 16). As such, despite a total of only 9 studies reported to date (14-22) on *in-vivo* 1H-MRS of 2HG in gliomas including 2 animal studies (20, 22), 5 different 1H-MRS methods were already explored.

In this review, we first summarize the biochemistry of 2HG and its significance in the diagnosis of IDH-MT gliomas. Secondly, we comparatively review 1H-MRS methods and findings in the previous studies. Finally, we discuss the current status of 1H-MRS in the diagnosis of IDH-MT gliomas as a technical guideline for neuroradiologists.

Received February 3, 2016; accepted after revision June 2, 2016.
This study was supported by a grant from the Ministry for Health, Welfare & Family Affairs (HI13C0015) in Korea, and by a grant from Seoul National University College of Medicine (800-20130068).
Corresponding author: Hyeonjin Kim, PhD, Department of Radiology, Seoul National University Hospital, 101 Daehak-ro, Jongno-gu, Seoul 03080, Korea.
• Tel: (822) 740-8543 • Fax: (822) 743-6385
• E-mail: hyeonjinkim@snu.ac.kr

Korean Journal of Radiology
KJR

Altered Metabolism and Overproduction of 2HG in IDH-MT Gliomas and Their Significance in Noninvasive Detection of 2HG by 1H-MRS

Isocitrate dehydrogenase is an enzyme with three isoforms, i.e., IDH1, IDH2, and IDH3 (13). Intra-cellularly, it catalyzes the oxidative decarboxylation of isocitrate to α-ketoglutarate (α-KG) in cytoplasm and peroxisomes (IDH1) and in mitochondria (IDH2 and IDH3) (Fig. 1) (13, 23). Highly frequent mutations in IDH1 and IDH2 genes are reported in low grade gliomas and secondary glioblastomas (10, 11). These mutations result in altered enzymatic activities of IDH1 and IDH2 such that they catalyze the reduction of α-KG to 2HG (12) instead of facilitating the production of the former (Fig. 1). As it is an aberrant product arising from altered metabolism in IDH-MT gliomas, 2HG is designated as an onco-metabolite (13, 24).

In IDH-MT gliomas, 2HG accumulates to a similar or higher level than 1H-MRS-visible brain metabolites, and 2–3 orders of magnitude higher than in IDH-WT gliomas or normal brain tissue (13). Thus, 1H-MRS has the potential to quantify 2HG non-invasively and discriminate IDH-MT gliomas from IDH-WT gliomas as well as normal tissue. Thus, 1H-MRS can directly determine the mutational status of gliomas non-invasively. The substantial difference in the frequency of IDH-mutational status between primary and secondary glioblastomas (11) further contributes to the potential diagnostic efficacy of 1H-MRS of 2HG (24). In cases where 2HG content correlates with tumor cellularity, 1H-MRS of 2HG can be used for guiding biopsy and surgery (15, 18), and monitoring treatment response (16). In addition, the longer survival duration of patients with IDH-MT gliomas than IDH-WT gliomas (11) also suggests a potential prognostic value of 1H-MRS of 2HG. These characteristics distinguish 2HG from previously proposed brain metabolites as 1H-MRS-etectable biomarkers of gliomas (1, 2, 6).

Recent findings also emphasize the potential importance of other brain metabolites in IDH-MT gliomas. For instance, the carbon source of 2HG is derived from glutamine (Gln) (12), and the reduction of glutamate (Glu) levels may be associated with the pathogenesis of the IDH1-MT gliomas (25, 26). Also, the down-regulation of glutathione (GSH) in IDH1-MT gliomas is proposed as a potential therapeutic target (27). Therefore, developing 1H-MRS methods that allow for more comprehensive metabolic profiling can play a pivotal role for better understanding the pathogenesis and progression of the diseases such as whether the oncogenesis is directly associated with 2HG or a consequence of the subsequent metabolic alterations. It may also shed light

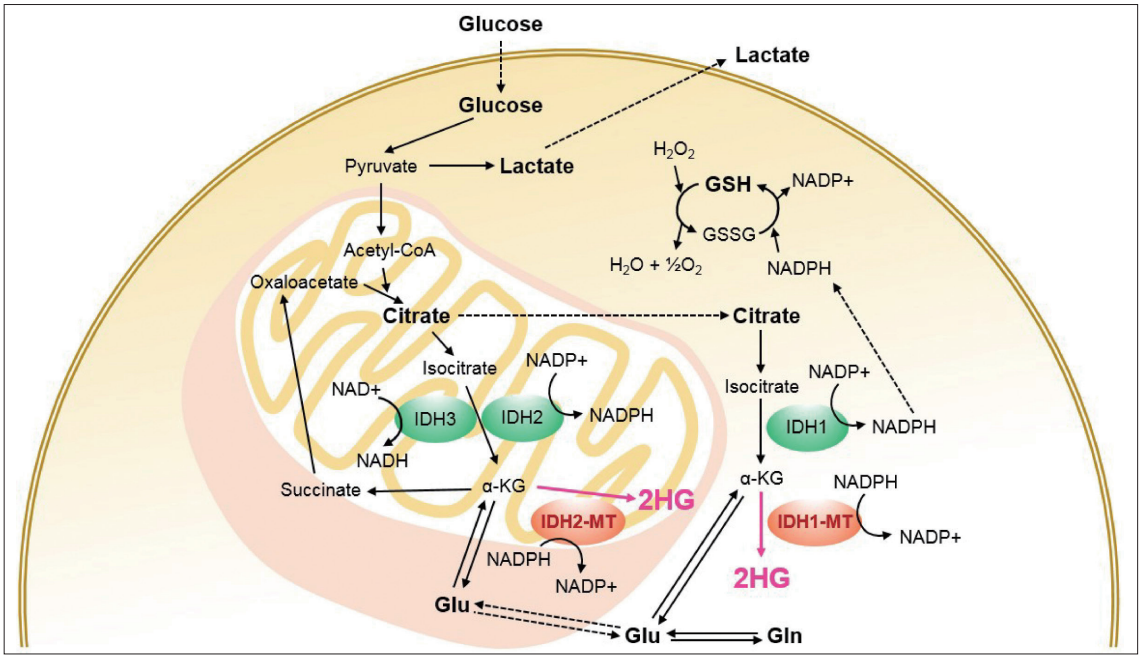

Fig. 1. Simplified metabolic pathways associated with isocitrate dehydrogenase (IDH) and 2-hydroxyglutarate (2HG). Mutations of IDH1 and IDH2 result in overproduction of 2HG. 1H-MRS-visible metabolites including 2HG are marked in bold. Acetyl-CoA = acetyl coenzyme A, Gln = glutamine, Glu = glutamate, GSH = glutathione, GSSG = glutathione disulfide, H_2O = water, H_2O_2 = hydrogen peroxide, IDH-MT = mutant isocitrate dehydrogenase, NAD = nicotinamide adenine dinucleotide, NADH = nicotinamide adenine dinucleotide hydrate, NADP = nicotinamide adenine dinucleotide phosphate, NADPH = nicotinamide adenine dinucleotide phosphate hydrate, α-KG = alpha-ketoglutarate

on the underlying mechanism of longer survival of patients with IDH-MT glioma vs. IDH-WT gliomas (20, 25-27), and the development of novel therapeutic strategies (26-28).

Spectral Characteristics of 2HG and Its Background Metabolites

The 2HG molecule has 5 non-exchangeable protons (5-spin system) with complicated J-coupling interactions (16). These interactions refer to inter-spin interactions through electron bonds in a molecule (29, 30). Such an indirect interaction between spins rather than a direct interaction through space is termed as J-coupling and the spins involved in the interaction are said to be J-coupled (29, 30). J-coupling results in peak splitting (e.g., a singlet into a multiplet) and changes in line shape and signal amplitude as a function of time (typically, echo time [TE]), namely J-evolution (29, 30). Different spin systems undergo different J-evolution depending on their coupling networks and coupling strength expressed as a J-constant in Hz (29, 30). The majority of the 1H-MRS-detectable metabolites have coupled spins such as 2HG, Glu, Gln, gamma-aminobutylic acid (GABA), and N-acetylaspartylglutamate (NAAG) (31). On the other hand, water and creatine (Cr) are representative metabolites with uncoupled spins only. The spectral characteristics of 2HG are determined by J-coupling in combination with the resonance frequencies of the 5 protons that are determined by chemical environments of the protons in the molecule (chemical-shift), giving rise to three multiplets at 3T centered at ~4.0, ~2.3, and ~1.9 ppm (contributed by 1, 2, and 2 spins, respectively) (Fig.

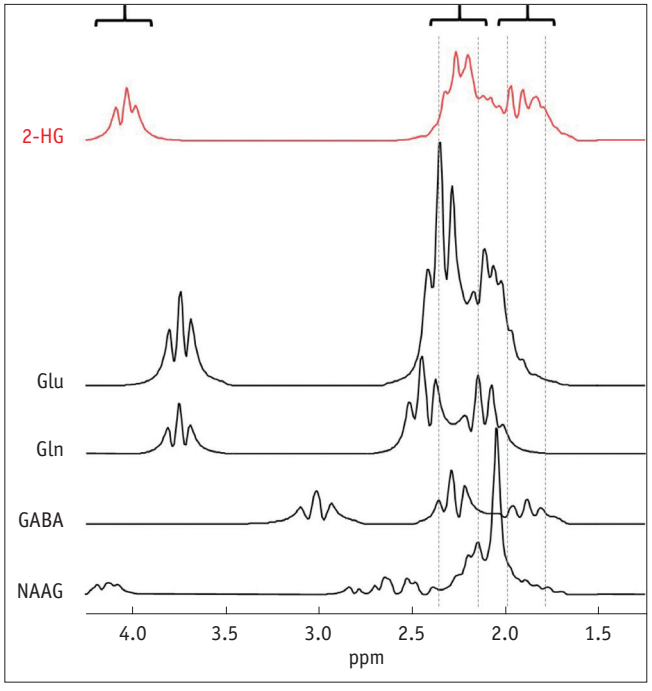

Fig. 2. Simulated spectra of 2HG and its background metabolites at 3T. Concentration ratio of 5:9.25:4.5:1.5:1.5 (mM) was assumed for 2HG:Glu:Gln:GABA:NAAG. Linewidth of all spectra were broadened to mimic *in-vivo* spectra. GABA = gamma-aminobutylic acid, Gln = glutamine, Glu = glutamate, NAAG = N-acetylaspartylglutamate, 2HG = 2-hydroxyglutarate

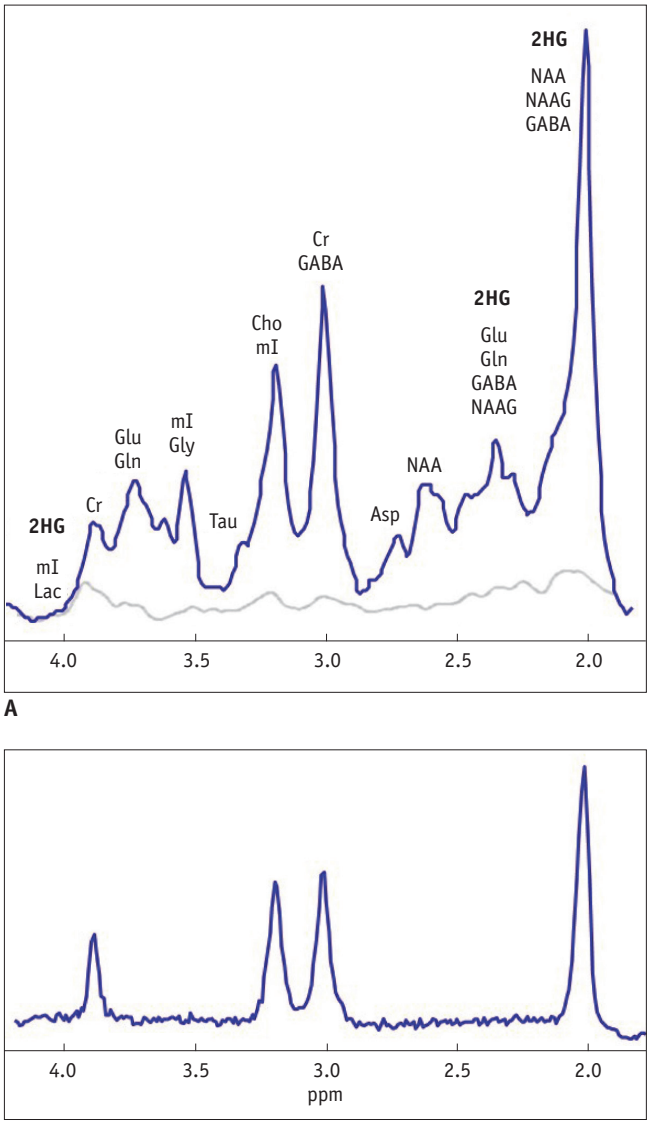

Fig. 3. Representative *in-vivo* spectra of normal human brain at 3T acquired at short TE (A) and long TE (B). Spectral baseline is also illustrated in **A**, which is typically assumed to be negligible in **B**. In **B**, spectrum consists mainly of Cr (~3.0 and ~3.9 ppm), Cho (~3.2 ppm), and NAA (~2.0 ppm) signals. Spectral locations of 2HG are also shown. Asp = aspartate, Cho = choline, Cr = creatine, GABA = gamma-aminobutylic acid, Gln = glutamine, Glu = glutamate, Gly = glycine, Lac = lactate, mI = myo-inositol, NAA = N-acetylaspartate, NAAG = N-acetylaspartylglutamate, Tau = taurine, TE = echo time, 2HG = 2-hydroxyglutarate

Korean Journal of Radiology
KJR

2) (16). The spins resonating at ~1.9 ppm are J-coupled with the spin resonating at ~4.0 ppm and also with those resonating at ~2.3 ppm (16). The multiplet at ~4.0 ppm is relatively small in amplitude as it is contributed by only one proton, overlaps with signals from lactate (Lac) and myo-inositol (mI) (Fig. 3), and is close to the strong Cr (~3.9 ppm) and water (~4.7 ppm) signals. The multiplet at ~1.9 ppm also overlaps with signals from other metabolites (Fig. 2), in particular, with N-acetylaspartate (NAA) (Fig. 3). The multiplet at ~2.3 ppm has the largest signal and is therefore widely used as a target signal for 2HG quantification (Fig. 2). However, it also severely overlaps with signals from at least 4 other metabolites (Figs. 2, 3) (15, 16).

Short TE, Long TE, Difference Editing and 2D Methods, and Data Post-Processing

Short TE

In a short TE method, spectra are acquired at a shortest TE attainable in order to minimize signal loss resulting from relaxation and, for coupled spins, J-evolution. For a PRESS sequence (32) that is one of the most widely used single-voxel 1H-MRS pulse sequences together with a STEAM sequence (33) at clinical field strength, a shortest TE can slightly differ for different MR scanners depending on the design of radio-frequency (RF) and gradient pulses, but is ~30 ms at 3T. At a shortest TE, all metabolite signals are maximized, which is of great advantage in terms of SNR of spectra and thus scan time. A short TE method does not require any modification of vendor-provided pulse sequences, hence is most commonly used in 1H-MRS in combination with spectral fitting for quantification of individual metabolites.

However, a shortest TE maximizes not only the target signal of 2HG at ~2.3 ppm but also those background signals from Glu, Gln, GABA, and NAAG (Fig. 2). The resulting severe spectral overlap is exacerbated by the presence of spectral baseline that is also maximized at the shortest TE (Fig. 3). Spectral baseline is contributed mainly by macromolecules (MMs) such as proteins and peptides (34), and also by lipid (35, 36). MMs also have J-coupled spins and their T1 and T2 are short relative to metabolites (34). The influence of spectral baseline on the quantitative analysis of spectra acquired at a shortest TE is well documented (37, 38). In particular, quantification of Glu and Gln is most influenced by spectral baseline among the 1H-MRS-visible metabolites (37). As the target signal of 2HG at ~2.3 ppm directly overlaps with Glu and Gln, the quantification of 2HG by using a short TE method can be very challenging, sometimes resulting in false 2HG-positive or 2HG-negative cases, as previously demonstrated (14, 15, 17). For this reason, different 1H-MRS methods were explored in the previous 1H-MRS 2HG studies such as a long TE method (16, 17, 19, 21), a difference editing (15, 16), and a 2-dimensional (2D) method (15).

To minimize its influence on the quantitative outcome, spectral baseline can be modeled based on metabolite-nulled spectra as a surrogate of true spectral baseline, which are acquired with T1-weighting by taking advantage of the substantially short T1 of MMs relative to those of metabolites (35, 37). The modeled spectral baseline is then incorporated into the spectral fitting. A better but more time-consuming approach is to acquire such a metabolite-nulled spectrum in a subject-specific manner (39, 40).

Long TE

A long TE method, which is a simplest practice of 'spectral editing', takes advantage of different J-evolution of different coupled spin systems (30, 41). It also takes advantage of different T2 between metabolites and spectral baseline (41). Using J-evolution and T2 as 'spectral contrast', spectra can be 'edited' for discriminating a target signal from background signals, and the integrity of the edited target signal is determined by how precisely the long TE is tuned.

In fact, a long TE method has long been used for 1H-MRS of gliomas, for instance, for the quantification of Cr and choline (Cho) (Fig. 3) (7). A long TE does not need to be fine-tuned for such singlets from uncoupled spins. It is simply optimized by making it as long as possible such that spectral baseline and background metabolite signals from coupled spins are effectively suppressed, while retaining an observable amount of signal from the target singlet(s) (Fig. 3). However, for spectral editing of a target metabolite with coupled spins against background metabolites also with coupled spins, thorough analyses of the evolution of all spin systems involved are required for optimization of TE (41, 42). For a simple coupled spin system, this can be achieved by analytically calculating the spin evolution using product operators (43) assuming that all RF pulses are applied instantaneously (29, 43). For instance, for the Lac spin system, the J-evolution of the doublet at ~1.3 ppm can be approximated simply with a cos ($\pi \cdot J \cdot TE$) term, where J is the J-constant between the coupled spins (=

6.93 Hz for Lac) (29). However, for more complicated spin systems such as 2HG, Glu, and Gln, analytic solution of spin evolution is difficult and requires numerical calculation (42, 44, 45) or investigation at least in phantom. This approach can also incorporate the intra-pulse spin evolution particularly during slice selection (42, 44, 45). The signal yield of coupled spins can substantially differ for different combinations of TE1 and TE2 for a given total TE (= TE1 + TE2) with a PRESS sequence (41, 46). Also, to minimize the signal loss of a target signal and maximize the suppression of spectral baseline, an optimal total TE is chosen as ≥ ~100 ms at 3T (16, 19, 41). Optimal TE facilitates great improvement of the signal-to-background ratio of a target signal at the cost of its SNR, which is the primary purpose of spectral editing (41).

While a long TE method may provide an effectively isolated target signal, it is subject to quantitative error due to T2 relaxation, which may be altered in the diseased brain or in the progression of diseases (21, 47). Also, a long TE method with a PRESS sequence may require pulse sequence modification for individually adjustable TE1 and TE2.

Difference Editing

A difference editing method utilizes J-coupling as spectral contrast as in the long TE method, and has long been used in glioma for Lac editing against lipid that also has the major signal at ~1.3 ppm (48). Recalling that the J-evolution of the Lac doublet at ~1.3 ppm can be approximated by cos ($\pi \cdot J \cdot TE$) with J = 6.93 Hz, the Lac signal is inverted at TE = 1/J = 144 ms (because cos (π) = -1), and evolves back to positive signal at TE = 2/J = 288 ms (because cos (2π) = 1) (48). By subtracting the former from the latter, the target spectral region of the resulting 'difference' spectrum is contributed mainly by Lac (48). Alternative to this approach using two different TEs, frequency-selective RF pulses (a pair of editing pulses) can be used for difference editing, often with a set of spoiling gradient pulses (49-51). In the case of 2HG (15, 16), the editing pulses are tuned at ~1.9 ppm, and yet indirectly influence the line shape of the multiplet at ~4.0 ppm due to J-coupling between the spins contributing to the two multiplets (Fig. 4). By subtracting the two spectra acquired at the same TE but with and without the editing pulses from each other, the target spectral region (~4.0 ppm) in the difference spectrum consists mainly of the signal from 2HG (Fig. 4). Note that although the 2HG signal at ~4.0 ppm has spectral overlap with Lac and mI, those Lac and mI spins responsible for the signals at this target spectral region do not have their J-coupled counterpart spins resonating in the vicinity of ~1.9 ppm (15, 16). Therefore, their signals at the target spectral region are canceled out by subtraction.

In difference editing, the pulse sequence optimization

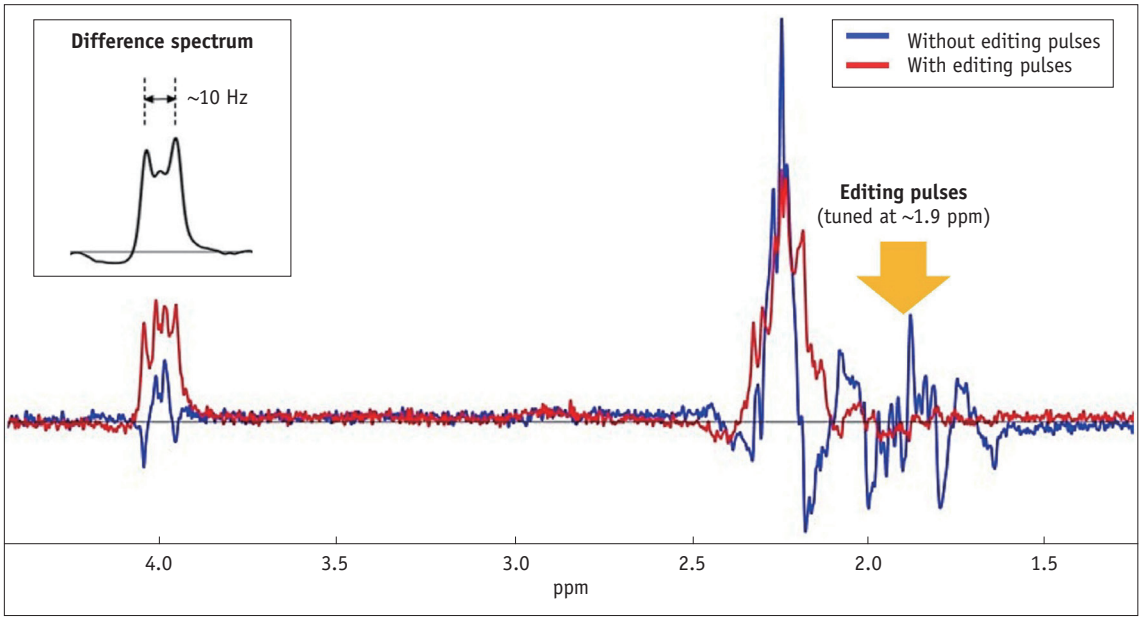

Fig. 4. Illustration of basic principle of difference editing method for 2HG editing in phantom at 3T. Spectra acquired with and without editing pulses that are tuned at ~1.9 ppm are shown in red and blue, respectively. By subtracting latter from former, edited 2HG signal is obtained at ~4.0 ppm in difference spectrum (shown in inset), which appears as doublet. Note that peak-to-peak distance of edited 2HG doublet is ~10 Hz at 3T. 2HG = 2-hydroxyglutarate

Korean Journal of Radiology
KJR

requires finding a TE that can yield a maximum signal after subtraction. In the case of using editing pulses, the choice of a TE is subject to the duration of the editing pulses, which are much longer than those pulses for spatial localization to achieve high spectral selectivity (15, 16). As such, the total TE is also indispensably long, which may therefore be subject to quantification errors inherent to long TE method. The difference spectra cannot provide comprehensive metabolic profiles. However, the spectrum acquired without the editing pulses may be used instead. As it requires subtraction of spectra with a relatively long scan time, all difference spectra methods are particularly subject to patient motion (29). For 2HG, the subtracted 2HG signal at ~4.0 ppm appears a doublet (Fig. 4), and the peak-to-peak distance of the doublet is very useful for examining the integrity of the edited 2HG signal. This is particularly so, given the spectral proximity of the target signal of 2HG to the strong water signal. A basic pulse sequence for difference editing is available commercially. For instance, in Siemens, a generic PRESS sequence can be used in combination with a MEGA module (49) implemented in the sequence for additional suppression of water and lipid. The frequency of the editing pulses needs to be adjusted accordingly, and for optimization of TE1 and TE2 separately it may also require sequence modification as with a long TE PRESS sequence.

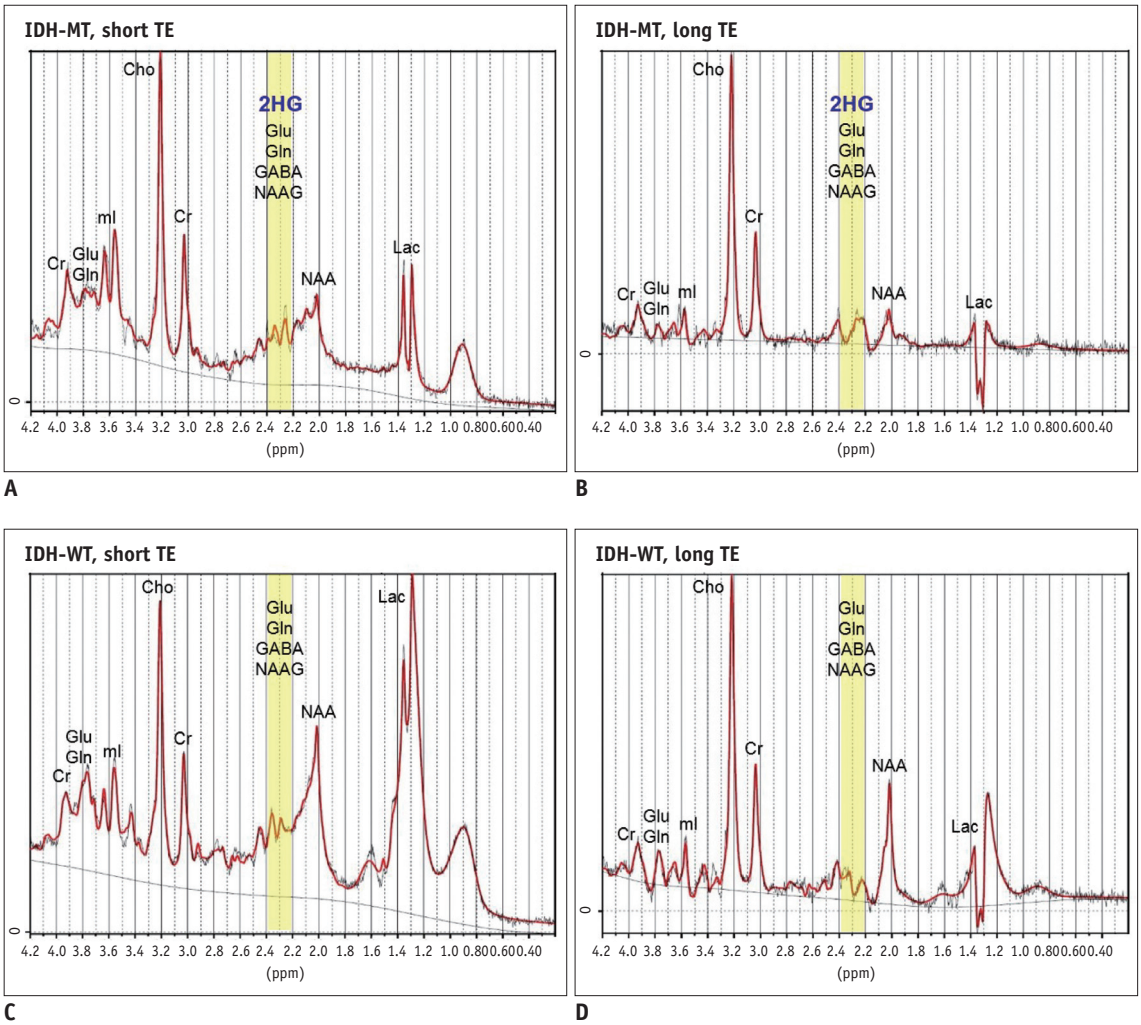

Fig. 5. Representative brain spectra of glioma patients by using short TE and long TE methods at 3T.
Spectra from IDH-MT glioma patient **(A, B)** are compared with those from IDH-WT glioma patient **(C, D)**. For all spectra, correct diagnostic results were obtained by LCModel (i.e., 2HG-positive for **A** and **B**, and 2HG-negative for **C** and **D**). Compared to spectra from normal human brain (Fig. 3), Cho/NAA ratios were substantially increased in these glioma patients. Cho = choline, Cr = creatine, GABA = gamma-aminobutylic acid, Gln = glutamine, Glu = glutamate, IDH-MT = isocitrate dehydrogenase-mutated, IDH-WT = isocitrate dehydrogenase wild-type, Lac = lactate, mI = myo-inositol, NAA = N-acetylaspartate, NAAG = N-acetylaspartylglutamate, TE = echo time, 2HG = 2-hydroxyglutarate

2D

Two-dimensional methods are in use for high resolution nuclear magnetic resonance to identify the J-coupling network of spin systems (peak assignment) (52). The extension of the dimension of spectra is achieved by two time variables in the sequence-one for the time between the excitation and the onset of data acquisition (t_1) and the other for the duration of data acquisition period (t_2). For instance, in the correlation spectroscopy (52, 53), signal is acquired during the t_2 period as in one-dimensional spectroscopy, but repetitively with different t_1 values. The resulting spectra are expressed on a 2D frequency space (f_1, f_2) via the 2D fast Fourier transformation of the signal, S (t_1, t_2). The resolution of the spectra is determined not only by the number of data points during t_2 period, but also by the number of experiments with different t_1 values. Among the peaks in the diagonal ($f_1 = f_2$) and off-diagonal regions of the spectra, those off-diagonal peaks or cross-peaks provide information on correlations (J-coupling) between peaks, and therefore allow for unambiguous assignment of peaks (53). However, due to the long acquisition time required to obtain reasonable spectral resolution, the *in-vivo* application of 2D-MRS is limited only when a target spectral region is severely crowded with background signals as in the case with 2HG (15). Also, a 2D pulse sequence is usually unavailable in clinical scanners, and the method requires additional data post-processing for metabolite quantification (15).

Finally, optimal sequence parameters (e.g., TE) can differ for different designs of RF and gradient pulses, and at different field strength. Therefore, sequence optimization needs to be performed for the given MR scanner and pulse sequence.

Data Post-Processing

The LCModel (38, 54) is currently the most widely used 1H-MRS data post-processing software package, which performs spectral fitting in frequency-domain. The current version of LCModel employs an extended spectral basis set including modeled MMs and lipids (35, 36, 54, 55), and therefore does not require a priori knowledge about spectral baseline. The MRUI (56) is another frequently used software package for metabolite quantification, which employs time-domain analysis. In general, one of such software packages is necessary for metabolite quantification for spectra obtained by a short TE method. For those edited spectra, spectral fitting may not be necessary if the target signal is effectively isolated from its background signals. The precision of spectral fitting is typically reported for individual metabolites in terms of the Cramer-Rao-Lower-Bound (CRLB) that sets a lower bound on the variance of the fitting estimate (44, 57). A CRLB of ≤ 20% is often used to indicate successful fitting (11, 12, 15, 22, 29).

The representative spectra from IDH-WT and IDH-MT glioma patients obtained by short TE and long TE methods are shown in Figure 5, for which LCModel was used for data post-processing.

Reviews on *In-Vivo* 1H-MRS Studies in IDH-MT Gliomas

The 1H-MRS methods for identifying IDH-mutational status in gliomas in the previous *in-vivo* studies are summarized in Table 1.

Short TE

Pope et al. (14) report 100% sensitivity and 74% specificity of a short TE method, in 9 IDH-MT and 15 IDH-WT glioma patients with 4 false positive cases. The 2HG concentrations as measured by 1H-MRS and liquid chromatography-mass spectrometry (LC-MS) are highly correlated ($r^2 > 0.56$); but 2HG concentrations (LC-MS) are not correlated with tumor grades. Andronesi et al. (15) compare performance of a short TE method to difference editing and 2D methods; while sensitivity and specificity are not reported, limited performance of a short TE method is shown, wherein 3 spectra from 2 healthy voxels and 1 IDH-WT tumor voxel result in false positive cases (including one case with CRLB > 20% from a healthy subject). Choi et al. (17) show a 77% sensitivity and 100% specificity for a short TE method in comparison to a long TE method. In a study on 1H-MRS performance in patients, Natsumeda et al. (18) report 100% sensitivity and 72% specificity where a 2HG cutoff concentration of 1.489 mM is used in differentiation between 2HG-positive and -negative cases in consideration of the limited SNR of 1H-MRS. In this study, 10 of 25 data (40%) from IDH-MT glioma patients and 9 of 27 data (33%) from IDH-WT glioma patients are excluded according to the data exclusion criteria based on the resulting 2HG concentrations and respective CRLB values. Interestingly, the survival rate of the IDH-MT glioma patients is significantly higher than the IDH-WT glioma patients (80% vs. 44.4%), corroborating previous reports (11); in addition, patients with high 2HG concentrations (>

Table 1. 1H-MRS Methods and Their Performance in Identifying IDH-Mutational Status in Gliomas

Method	Authors (Ref)	Subject	Number of Subjects (Number of Voxels)*			Sensitivity (%)	Specificity (%)†	Analysis Software	Cutoff CRLB (%)‡	Reference Peak	Scanner	Field Strength (T)	Number of Channels	Pulse Sequence	TR/TE (TE1, TE2) (ms)	Scan Time (min)	Voxel Volume (cm^3)
			MT	WT	Healthy												
Short TE	Andronesi et al. (15)	Human	2	4	4	NA	NA	LCModel	20	Glu + Gln	Siemens	3.0	32	LASER	1500/45	3.2	27.0, 42.8
	Choi et al. (17)	Human	22	-	7	77	100	LCModel	19	Water	Philips	3.0	8	PRESS	2000/35 (21, 14)	4.3	8.0
	Pope et al. (14)	Human	9	15	-	100	73	LCModel	NA	Water, Cr	Siemens	3.0	12	PRESS	2000/30	4.3	8.0
	Natsumeda et al. (18)	Human	25 (15)	27 (18)	-	100	72	LCModel	35§	Water	GE	3.0	8	PRESS	1500/30	3.2–4.9	(1.2–2.0)^3
	Lazovic et al. (20)	Mouse	8	7	-	100	100	LCModel	20	Cho	Bruker	7.0	1	PRESS	4000/6.9	34.1	3.0
Short TE with baseline	Heo et al. (22)	Rat	7 (7)	6 (6)	(6)	100	83	MRUI	20	Water	Agilent	9.4	1	SPECIAL	4000/2.8	25.6	9.6 x 10^{-3}
Long TE	Choi et al. (16)	Human	15	15	-	100	100	LCModel	19	Water	Philips	3.0	8	PRESS	2000/97 (32, 65)	2.1	8.0
	Choi et al. (17)	Human	22	-	7	100	100	LCModel	19	Water	Philips	3.0	8	PRESS	2000/97 (32, 65)	4.3	8.0
	de la Fuente et al. (19)	Human	22	6	-	91	100	LCModel	30‖	Water	GE	3.0	8	PRESS	2000/97 (26, 71)	5.5–9.5	8.0
	Emir et al. (21)	Human	10 (10)	4 (4)	8 (25)	NA	93	LCModel	30	Water	Siemens	7.0	32	Semi-LASER	5000–6000/110	10.7–12.8	8.0
Difference editing	Andronesi et al. (15)	Human	2	4	4	NA	NA	MRUI	20	Glu + Gln	Siemens	3.0	32	MEGA-LASER	1500/75	5.0	27.0, 42.8
	Choi et al. (16)	Human	NA	NA	NA	100	100	LCModel	NA	Water	Philips	3.0	8	MEGA-PRESS	2000/106 (26, 80)	13.0	8.0
2D	Andronesi et al. (15)	Human	2	4	4	NA	NA	Matlab	NA	Glu + Gln	Siemens	3.0	32	LASER-COSY	1500/45	12.8	27.0, 42.8

*Number of voxels can be different from number of subjects by excluding data with poor quality or by acquiring more data from different regions of brain of same subject, †Specificity: estimated from IDH wild-type tumor voxels + healthy voxels, ‡Cutoff Cramer-Rao lower bound for successful spectral fitting, §For 2HG concentrations of > 1 mM, ‖For 2HG concentrations of ≥ 1 mM. Cho = choline, Cr = creatine, Gln = glutamine, Glu = glutamate, healthy = healthy brain tissue, IDH = isocitrate dehydrogenase, MT = tissue from IDH-mutated tumor, NA = not available, sensitivity = estimated from IDH-mutated tumor voxels, TE1 = 1st echo time, TE2 = 2nd echo time, TR = repetition time, WT = tissue from IDH wild-type tumor, 1H-MRS = proton magnetic resonance spectroscopy, 2HG = 2-hydroxyglutarate

1.489 mM) show a longer overall survival trend than those with low 2HG concentrations.

The performance of a short TE method is also tested in animal models at high field (20, 22). Given the heterogeneity of gliomas in humans, the use of animal models can provide a better comparison between the study cohorts with and without IDH-mutation (20). Lazovic et al. (20) report 100% sensitivity and specificity at 7T in mouse glioma models using human U87 glioma cells overexpressing IDH1-mutation. Such excellent performance of a short TE method most likely results from higher spectral SNR and dispersion of the spectra at high field, large voxel size and number of signal averages, and high 2HG concentrations (10–20 mM) in the animal models. Additionally, diffusion, perfusion, and T2-weighted (T2-mapping) MRI scans show no significant difference in the respective MRI measures between the animal groups with and without IDH-mutation. Using rat models of IDH1/2-mutant-overexpressing F98 glioma, Heo et al. (22) also describe the challenges with 1H-MRS of 2HG even at 9.4T. Given that spectral baseline is the primary factor hindering the differentiation between Glu and Gln (37, 38), that the main signal of 2HG directly overlaps with these metabolites, and that measured spectral baseline provides better information than those modeled (39, 40), they investigated the performance of a short TE method in combination with voxel-specifically measured spectral baseline, and report 100% sensitivity and 83% specificity.

Overall, the reported sensitivity and specificity of a short TE method ranges 77–100% and 72–100%, respectively, and there is a trend towards lower specificity than sensitivity. Despite the severe spectral overlaps, these results support the potential applicability of 1H-MRS in the non-invasive detection of 2HG. However, the reported limitation of the short TE method should be noted.

Long TE

Choi et al. (16, 17) report 100% sensitivity and specificity in two different patient studies with a long TE method. In comparison to a short TE method, the long TE method improves the sensitivity from 77% to 100% (17). Using a long TE method, de la Fuente et al. (19) investigate the impact of voxel size on the detectability of 2HG. Three different voxel sizes of < 3.4 mL, ≥ 3.4 and < 8 mL, and ≥ 8 mL result in 8% (2/24), 47% (16/34), and 91% (20/22) sensitivity. Also, 6 of the 6 voxels (voxel size ≥ 8 mL) from IDH-WT gliomas do not show 2HG signal at the target spectral region. In this study, 2HG concentrations are correlated with tumor cellularity but not with the degree of tumor cell proliferation. Importantly, 2HG levels gradually reduce following treatment with radiation and chemotherapy. A long TE method is also tested at 7T by Emir et al. (21) where the specificity from 29 healthy or IDH-WT glioma tissue is 93% (sensitivity data not shown explicitly). Although a small number of voxels is used, the 2HG concentrations are higher in IDH2-MT gliomas (n = 3) than in IDH1-MT gliomas (n = 7) in that study.

Overall, the reported sensitivity and specificity with a long TE method are ~90–100% for both, and appear better than those with a short TE method, most likely due to the effective isolation of the target 2HG signal and negligible contribution from spectral baseline at a total TE of ~100 ms (16, 17). However, as discussed by the authors (16, 17, 21), the resulting 2HG content may be prone to quantitative errors resulting from signal loss due to relaxation. The signal loss arising from a long TE may also hinder the quantification of other metabolites in the edited spectra (21).

Difference Editing and 2D

Using a difference editing method (49), Choi et al. (16) acquire spectra from 7 subjects with either IDH-MT or -WT gliomas. Although the mutational status of the patients is not given explicitly, the diagnostic outcome with difference editing is comparable to a long TE method with 100% sensitivity and specificity. Andronesi et al. (15) also test a difference editing method (49) together with a 2D method in 10 humans including 2 IDH-MT glioma patients. In their study, the mean 2HG levels (normalized to Glu + Gln) from IDH-WT voxels are non-zero with both methods; however, they are substantially lower than with a short TE method.

To date, the performance of a difference editing method in IDH-MT gliomas is reported from only 2 studies with small numbers of subjects (15, 16)–only 1 study for a 2D method (15). However, given the effective isolation of a target signal provided by a difference editing method and the additional information for unambiguous peak assignment provided by a 2D method, these methods have potential applicability.

Alterations in the Concentrations of Other Metabolites in IDH-MT Gliomas

Pope et al. (14) report that voxels that result in the 4 false positive cases in their study have higher Glu and Gln levels than other IDH-WT voxels. This observation

Korean Journal of Radiology
KJR

emphasizes the influence of the background signals on the quantification of 2HG in the spectral fitting. However, no difference in Glu and Gln concentrations are found between the study cohorts with and without IDH-mutation as measured by LC-MS. In contrast to these findings, Choi et al. (17) report reduced Glu and elevated Gln levels in IDH-MT gliomas relative to IDH-WT gliomas, but with no correlations with 2HG levels. Several other studies also report altered Glu and/or Gln levels in IDH-MT glioma patients (e.g., significantly lower Glu + Gln (18) and a trend of lower Glu (21)) and animal models (e.g., lowered Glu/Cho ratio (20)).

Significantly lowered GSH concentrations (14, 18) as well as a trend of lower GSH (21) are also reported in IDH-MT glioma patients. This may be due to reduced nicotinamide adenine dinucleotide phosphate hydrate as a result of IDH-mutation, which is involved in the regeneration of the reduced form of GSH, and therefore may potentially be associated with the pathogenesis and progression of the IDH-MT gliomas (14). In an animal study, however, there is no difference in GSH concentrations normalized to Cho between the animal groups with and without IDH-mutation (20). Pope et al. (14) also report high Cho/Cr ratios in IDH-MT gliomas relative to those in IDH-WT gliomas, and suggest increased cell density from IDH-mutation-mediated cell proliferation as a probable cause. In addition, Emir et al. (21) report trends of lower citrate, mI, Cho and Cr, and higher Lac, NAA + NAAG and glucose + taurine in IDH-MT glioma patients than in IDH-WT glioma patients.

These *in-vivo* findings clearly need to be supported by further studies. Also, findings obtained at long TE may be prone to quantitative errors (16, 17, 21). Nonetheless, the altered Glu levels found in the majority of the *in-vivo* studies (17, 18, 20, 21) are in line with the previous findings (12, 58).

Data Inclusion/Exclusion Criteria and Presentation of 2HG Concentrations

Depending on their quality, spectra may need to be excluded prior to metabolite quantification. For instance, de la Fuente et al. (19) estimate the full-width-at-half-maximum (FWHM) of Cr signal, and those spectra with FWHM of Cr ≥ 0.08 ppm (~10 Hz at 3T) are excluded. However, even after such data screening, indeterminate diagnostic cases frequently occur after spectral fitting if the resulting CRLBs of 2HG are larger than a cutoff CRLB for successful fitting (e.g., CRLB ≤ 20%). To address this issue, various data inclusion/exclusion criteria are reported in terms of a detectable limit of 2HG concentrations in combination with a cutoff CRLB. For instance, Choi et al. (16) use 2HG concentrations ≥ 1.5 mM with CRLB < 18% as the inclusion criteria for 2HG-positive cases. Natsumeda et al. (18) use different criteria for different metabolites in consideration of their different concentrations and thus different SNR in the spectra. The experimental settings in the previous studies are quite diverse (Table 1), and consequently the reported detection limits of 2HG concentrations are also quite different (15, 16, 19), indicating the need for experimental setting-specific data inclusion/exclusion criteria.

Water signal is most widely used as an internal reference for the normalization of the 1H-MRS-measured concentrations of 2HG and other metabolites (14, 16-19, 21, 22). Water-normalized metabolite content can be further converted into absolute concentrations using a priori knowledge (16, 17, 19). Depending on the TE used for acquiring water-unsuppressed spectra, the water signal needs to be corrected for T2 relaxation (21). Alternatively, water-unsuppressed data need to be acquired using a STEAM sequence (17) which provides a shorter TE than a PRESS sequence. For spectra acquired at a long TE, T2 of metabolites can also be corrected based on the published data (16, 17, 19). In this procedure, however, care must be taken as different tumor types and grades can result in different T2 of water and other metabolites (21, 47). By using water content as a reference, the reported ranges of 2HG concentrations in IDH-MT glioma voxels in patients are: 1.7–8.9 mM (16), 2–15 mM (18), and 2–10 umol/g (21). In addition to water, Glu + Gln (15), Cr (14), and Cho (20) are also used as an internal reference. In particular, Andronesi et al. (15) propose normalization of 2HG by Glu + Gln based on their potential inter-relationship (12, 58), and report that a 2HG/(Glu + Gln) ratio of > 1 could be specific for IDH1-mutations.

CONCLUSION

In this review, we focused on technical aspects of previous *in-vivo* 1H-MRS studies of 2HG. Given that different experimental protocols were used with different data inclusion/exclusion criteria in the previous studies, and that there was a large inter-patient variability in reported 2HG content, the relative performance of the different 1H-MRS methods may be best compared in the same study

cohort with established procedures for screening, post-processing, interpretation and presentation of the data. 1H-MRS methods have individual pros and cons; hence, further technical development may be necessary in order to accurately quantify the target metabolite and better depict biochemical effects of mutation-dependent IDH activities as a consumer or producer of α-KG. However, as far as 'detection' of 2HG is concerned, these previous pioneering studies are in support of the diagnostic and prognostic potential of 1H-MRS in IDH-MT glioma patients. IDH-mutations and/or 2HG accumulations are recently identified in other cancers and disorders (59-66). Therefore, the efficacy of 2HG as a 1H-MRS biomarker of IDH-MT gliomas should also be investigated thoroughly (18).

Acknowledgments

The authors gratefully acknowledge Drs. Seung Hong Choi (Radiology), Chul-Kee Park (Neurosurgery), and Sunghyouk Park (Natural Product Research Institute) at Seoul National University/Hospital for sharing their expertise in the preparation of the manuscript.

REFERENCES

1. Law M, Yang S, Wang H, Babb JS, Johnson G, Cha S, et al. Glioma grading: sensitivity, specificity, and predictive values of perfusion MR imaging and proton MR spectroscopic imaging compared with conventional MR imaging. *AJNR Am J Neuroradiol* 2003;24:1989-1998
2. Möller-Hartmann W, Herminghaus S, Krings T, Marquardt G, Lanfermann H, Pilatus U, et al. Clinical application of proton magnetic resonance spectroscopy in the diagnosis of intracranial mass lesions. *Neuroradiology* 2002;44:371-381
3. Herholz K, Heindel W, Luyten PR, denHollander JA, Pietrzyk U, Voges J, et al. In vivo imaging of glucose consumption and lactate concentration in human gliomas. *Ann Neurol* 1992;31:319-327
4. Rock JP, Scarpace L, Hearshen D, Gutierrez J, Fisher JL, Rosenblum M, et al. Associations among magnetic resonance spectroscopy, apparent diffusion coefficients, and image-guided histopathology with special attention to radiation necrosis. *Neurosurgery* 2004;54:1111-1117; discussion 1117-1119
5. Verma N, Cowperthwaite MC, Burnett MG, Markey MK. Differentiating tumor recurrence from treatment necrosis: a review of neuro-oncologic imaging strategies. *Neuro Oncol* 2013;15:515-534
6. Blüml S, Panigrahy A, Laskov M, Dhall G, Krieger MD, Nelson MD, et al. Elevated citrate in pediatric astrocytomas with malignant progression. *Neuro Oncol* 2011;13:1107-1117
7. Howe FA, Barton SJ, Cudlip SA, Stubbs M, Saunders DE, Murphy M, et al. Metabolic profiles of human brain tumors using quantitative in vivo 1H magnetic resonance spectroscopy. *Magn Reson Med* 2003;49:223-232
8. Majós C, Alonso J, Aguilera C, Serrallonga M, Pérez-Martín J, Acebes JJ, et al. Proton magnetic resonance spectroscopy ((1) H MRS) of human brain tumours: assessment of differences between tumour types and its applicability in brain tumour categorization. *Eur Radiol* 2003;13:582-591
9. Zonari P, Baraldi P, Crisi G. Multimodal MRI in the characterization of glial neoplasms: the combined role of single-voxel MR spectroscopy, diffusion imaging and echo-planar perfusion imaging. *Neuroradiology* 2007;49:795-803
10. Parsons DW, Jones S, Zhang X, Lin JC, Leary RJ, Angenendt P, et al. An integrated genomic analysis of human glioblastoma multiforme. *Science* 2008;321:1807-1812
11. Yan H, Parsons DW, Jin G, McLendon R, Rasheed BA, Yuan W, et al. IDH1 and IDH2 mutations in gliomas. *N Engl J Med* 2009;360:765-773
12. Dang L, White DW, Gross S, Bennett BD, Bittinger MA, Driggers EM, et al. Cancer-associated IDH1 mutations produce 2-hydroxyglutarate. *Nature* 2009;462:739-744
13. Andronesi OC, Rapalino O, Gerstner E, Chi A, Batchelor TT, Cahill DP, et al. Detection of oncogenic IDH1 mutations using magnetic resonance spectroscopy of 2-hydroxyglutarate. *J Clin Invest* 2013;123:3659-3663
14. Pope WB, Prins RM, Albert Thomas M, Nagarajan R, Yen KE, Bittinger MA, et al. Non-invasive detection of 2-hydroxyglutarate and other metabolites in IDH1 mutant glioma patients using magnetic resonance spectroscopy. *J Neurooncol* 2012;107:197-205
15. Andronesi OC, Kim GS, Gerstner E, Batchelor T, Tzika AA, Fantin VR, et al. Detection of 2-hydroxyglutarate in IDH-mutated glioma patients by in vivo spectral-editing and 2D correlation magnetic resonance spectroscopy. *Sci Transl Med* 2012;4:116ra4
16. Choi C, Ganji SK, DeBerardinis RJ, Hatanpaa KJ, Rakheja D, Kovacs Z, et al. 2-hydroxyglutarate detection by magnetic resonance spectroscopy in IDH-mutated patients with gliomas. *Nat Med* 2012;18:624-629
17. Choi C, Ganji S, Hulsey K, Madan A, Kovacs Z, Dimitrov I, et al. A comparative study of short- and long-TE ^{1}H MRS at 3 T for in vivo detection of 2-hydroxyglutarate in brain tumors. *NMR Biomed* 2013;26:1242-1250
18. Natsumeda M, Igarashi H, Nomura T, Ogura R, Tsukamoto Y, Kobayashi T, et al. Accumulation of 2-hydroxyglutarate in gliomas correlates with survival: a study by 3.0-tesla magnetic resonance spectroscopy. *Acta Neuropathol Commun* 2014;2:158
19. de la Fuente MI, Young RJ, Rubel J, Rosenblum M, Tisnado J, Briggs S, et al. Integration of 2-hydroxyglutarate-proton magnetic resonance spectroscopy into clinical practice for disease monitoring in isocitrate dehydrogenase-mutant glioma. *Neuro Oncol* 2016;18:283-290
20. Lazovic J, Soto H, Piccioni D, Lou JR, Li S, Mirsadraei L, et al. Detection of 2-hydroxyglutaric acid in vivo by proton magnetic resonance spectroscopy in U87 glioma cells

overexpressing isocitrate dehydrogenase-1 mutation. *Neuro Oncol* 2012;14:1465-1472
21. Emir UE, Larkin SJ, de Pennington N, Voets N, Plaha P, Stacey R, et al. Noninvasive quantification of 2-hydroxyglutarate in human gliomas with IDH1 and IDH2 mutations. *Cancer Res* 2016;76:43-49
22. Heo H, Kim S, Lee HH, Cho HR, Xu WJ, Lee SH, et al. On the utility of short echo time (TE) single voxel 1H-MRS in non-invasive detection of 2-hydroxyglutarate (2HG); challenges and potential improvement illustrated with animal models using MRUI and LCModel. *PLoS One* 2016;11:e0147794
23. Yen KE, Bittinger MA, Su SM, Fantin VR. Cancer-associated IDH mutations: biomarker and therapeutic opportunities. *Oncogene* 2010;29:6409-6417
24. Esmaeili M, Vettukattil R, Bathen TF. 2-hydroxyglutarate as a magnetic resonance biomarker for glioma subtyping. *Transl Oncol* 2013;6:92-98
25. Chaumeil MM, Larson PE, Woods SM, Cai L, Eriksson P, Robinson AE, et al. Hyperpolarized [1-13C] glutamate: a metabolic imaging biomarker of IDH1 mutational status in glioma. *Cancer Res* 2014;74:4247-4257
26. Tönjes M, Barbus S, Park YJ, Wang W, Schlotter M, Lindroth AM, et al. BCAT1 promotes cell proliferation through amino acid catabolism in gliomas carrying wild-type IDH1. *Nat Med* 2013;19:901-908
27. Shi J, Sun B, Shi W, Zuo H, Cui D, Ni L, et al. Decreasing GSH and increasing ROS in chemosensitivity gliomas with IDH1 mutation. *Tumour Biol* 2015;36:655-662
28. Marin-Valencia I, Yang C, Mashimo T, Cho S, Baek H, Yang XL, et al. Analysis of tumor metabolism reveals mitochondrial glucose oxidation in genetically diverse human glioblastomas in the mouse brain in vivo. *Cell Metab* 2012;15:827-837
29. de Graaf RA. *In vivo NMR spectroscopy: principles and techniques*, 2nd ed. Chichester: John Wiley & Sons, 2007:26-32
30. Allen PS, Thompson RB, Wilman AH. Metabolite-specific NMR spectroscopy in vivo. *NMR Biomed* 1997;10:435-444
31. Govindaraju V, Young K, Maudsley AA. Proton NMR chemical shifts and coupling constants for brain metabolites. *NMR Biomed* 2000;13:129-153
32. Bottomley PA. Selective volume method for performing localized NMR spectroscopy. United States patent US 4480228. 1984 Oct 30
33. Frahm J, Bruhn H, Gyngell ML, Merboldt KD, Hänicke W, Sauter R. Localized high-resolution proton NMR spectroscopy using stimulated echoes: initial applications to human brain in vivo. *Magn Reson Med* 1989;9:79-93
34. Behar KL, Rothman DL, Spencer DD, Petroff OA. Analysis of macromolecule resonances in 1H NMR spectra of human brain. *Magn Reson Med* 1994;32:294-302
35. Seeger U, Klose U, Mader I, Grodd W, Nägele T. Parameterized evaluation of macromolecules and lipids in proton MR spectroscopy of brain diseases. *Magn Reson Med* 2003;49:19-28
36. Auer DP, Gössl C, Schirmer T, Czisch M. Improved analysis of 1H-MR spectra in the presence of mobile lipids. *Magn Reson Med* 2001;46:615-618
37. Hofmann L, Slotboom J, Jung B, Maloca P, Boesch C, Kreis R. Quantitative 1H-magnetic resonance spectroscopy of human brain: influence of composition and parameterization of the basis set in linear combination model-fitting. *Magn Reson Med* 2002;48:440-453
38. Provencher SW. Estimation of metabolite concentrations from localized in vivo proton NMR spectra. *Magn Reson Med* 1993;30:672-679
39. Cudalbu C, Mlynárik V, Gruetter R. Handling macromolecule signals in the quantification of the neurochemical profile. *J Alzheimers Dis* 2012;31 Suppl 3:S101-S115
40. Penner J, Bartha R. Semi-LASER 1 H MR spectroscopy at 7 Tesla in human brain: metabolite quantification incorporating subject-specific macromolecule removal. *Magn Reson Med* 2015;74:4-12
41. Kim H, Thompson RB, Hanstock CC, Allen PS. Variability of metabolite yield using STEAM or PRESS sequences in vivo at 3.0 T, illustrated with myo-inositol. *Magn Reson Med* 2005;53:760-769
42. Thompson RB, Allen PS. A new multiple quantum filter design procedure for use on strongly coupled spin systems found in vivo: its application to glutamate. *Magn Reson Med* 1998;39:762-771
43. Sørensen OW, Eich GW, Levitt MH, Bodenhausen G, Ernst RR. Product operator-formalism for the description of NMR pulse experiments. *Prog NMR Spectrosc* 1983;16:163-192
44. Young K, Govindaraju V, Soher BJ, Maudsley AA. Automated spectral analysis I: formation of a priori information by spectral simulation. *Magn Reson Med* 1998;40:812-815
45. Young K, Soher BJ, Maudsley AA. Automated spectral analysis II: application of wavelet shrinkage for characterization of non-parameterized signals. *Magn Reson Med* 1998;40:816-821
46. Thompson RB, Allen PS. Sources of variability in the response of coupled spins to the PRESS sequence and their potential impact on metabolite quantification. *Magn Reson Med* 1999;41:1162-1169
47. Li Y, Srinivasan R, Ratiney H, Lu Y, Chang SM, Nelson SJ. Comparison of T(1) and T(2) metabolite relaxation times in glioma and normal brain at 3T. *J Magn Reson Imaging* 2008;28:342-350
48. Lange T, Dydak U, Roberts TP, Rowley HA, Bjeljac M, Boesiger P. Pitfalls in lactate measurements at 3T. *AJNR Am J Neuroradiol* 2006;27:895-901
49. Mescher M, Merkle H, Kirsch J, Garwood M, Gruetter R. Simultaneous in vivo spectral editing and water suppression. *NMR Biomed* 1998;11:266-272
50. Rothman DL, Behar KL, Hetherington HP, Shulman RG. Homonuclear 1H double-resonance difference spectroscopy of the rat brain in vivo. *Proc Natl Acad Sci U S A* 1984;81:6330-6334
51. Hetherington HP, Avison MJ, Shulman RG. 1H homonuclear editing of rat brain using semiselective pulses. *Proc Natl Acad Sci U S A* 1985;82:3115-3118
52. Ernst RR, Bodenhausen G, Wokaun A. *Principles of nuclear magnetic resonance in one and two dimensions*. Oxford: Oxford

University Press, 1987:400-427
53. Aue WP, Bartholdi E, Ernst RR. Two-dimensional spectroscopy. Application to nuclear magnetic resonance. *J Chem Phys* 1976;64:2229-2246
54. Provencher SW. LCModel & LCMgui user's manual. Web site. http://s-provencher.com/pub/LCModel/manual/manual.pdf. Accessed January 5, 2016
55. Opstad KS, Bell BA, Griffiths JR, Howe FA. Toward accurate quantification of metabolites, lipids, and macromolecules in HRMAS spectra of human brain tumor biopsies using LCModel. *Magn Reson Med* 2008;60:1237-1242
56. Naressi A, Couturier C, Devos JM, Janssen M, Mangeat C, de Beer R, et al. Java-based graphical user interface for the MRUI quantitation package. *MAGMA* 2001;12:141-152
57. Cavassila S, Deval S, Huegen C, van Ormondt D, Graveron-Demilly D. Cramér-Rao bounds: an evaluation tool for quantitation. *NMR Biomed* 2001;14:278-283
58. Reitman ZJ, Jin G, Karoly ED, Spasojevic I, Yang J, Kinzler KW, et al. Profiling the effects of isocitrate dehydrogenase 1 and 2 mutations on the cellular metabolome. *Proc Natl Acad Sci U S A* 2011;108:3270-3275
59. Terunuma A, Putluri N, Mishra P, Mathé EA, Dorsey TH, Yi M, et al. MYC-driven accumulation of 2-hydroxyglutarate is associated with breast cancer prognosis. *J Clin Invest* 2014;124:398-412
60. Mardis ER, Ding L, Dooling DJ, Larson DE, McLellan MD, Chen K, et al. Recurring mutations found by sequencing an acute myeloid leukemia genome. *N Engl J Med* 2009;361:1058-1066
61. Struys EA, Salomons GS, Achouri Y, Van Schaftingen E, Grosso S, Craigen WJ, et al. Mutations in the D-2-hydroxyglutarate dehydrogenase gene cause D-2-hydroxyglutaric aciduria. *Am J Hum Genet* 2005;76:358-360
62. Green A, Beer P. Somatic mutations of IDH1 and IDH2 in the leukemic transformation of myeloproliferative neoplasms. *N Engl J Med* 2010;362:369-370
63. Ward PS, Patel J, Wise DR, Abdel-Wahab O, Bennett BD, Coller HA, et al. The common feature of leukemia-associated IDH1 and IDH2 mutations is a neomorphic enzyme activity converting alpha-ketoglutarate to 2-hydroxyglutarate. *Cancer Cell* 2010;17:225-234
64. Kang MR, Kim MS, Oh JE, Kim YR, Song SY, Seo SI, et al. Mutational analysis of IDH1 codon 132 in glioblastomas and other common cancers. *Int J Cancer* 2009;125:353-355
65. Sjöblom T, Jones S, Wood LD, Parsons DW, Lin J, Barber TD, et al. The consensus coding sequences of human breast and colorectal cancers. *Science* 2006;314:268-274
66. Lopez GY, Reitman ZJ, Solomon D, Waldman T, Bigner DD, McLendon RE, et al. IDH1(R132) mutation identified in one human melanoma metastasis, but not correlated with metastases to the brain. *Biochem Biophys Res Commun* 2010;398:585-587